Directly measuring the spatio-temporal electric field of focusing ultrashort pulses

Pamela Bowlan, Pablo Gabolde, and Rick Trebino

Georgia Institute of Technology, School of Physics
837 State St NW, Atlanta, GA 30332 USA
PamBowlan@gatech.edu

Abstract: We present the first technique for directly measuring (without assumptions) the spatio-temporal intensity and phase of a train of ultrashort pulses at and near a focus. Our method uses an experimentally simple and high-spectral resolution variant of spectral interferometry (SEA TADPOLE). To illustrate our technique, we measured the spatio-temporal electric field in and around the foci of several different types of lenses. To confirm our results, we also simulated these measurements by numerically propagating a pulse through each of the lenses used. From one set of measurements, we made a movie showing a focusing pulse with severe chromatic aberration.

OCIS codes: (320.7100) Ultrafast Measurements; (260.3160) Interference; (220.2560) Focus

References and links

1. M. Kempe, and W. Rudolph, "Impact of chromatic and spherical aberration on the focusing of ultrashort light pulses by lenses," Opt. Lett. **18**, 137-139 (1993).
2. M. Kempe, and W. Rudolph, "Femtosecond pulses in the focal region of lenses," Phys. Rev. A **48**, 4721-4729 (1993).
3. Z. Bor, "Distortion of femtosecond laser pulses in lenses," Opt. Lett. **14**, 119-121 (1989).
4. Ulrike Fuchs, Uwe D. Zeitner, and Andreas Tünnermann, "Ultra-short pulse propagation in complex optical systems," Opt. Express **13**, 9903-9908 (2005).
5. Dan Oron, and Yaron Silberberg, "Spatiotemporal coherent control using shaped, temporally focused pulses," Opt. Express **13**, 9903-9908 (2005).
6. Nirit Dudovich, Dan Oron, and Yaron Silberberg, "Single-pulse coherently controlled nonlinear Raman spectroscopy and microscopy," Nature **418**, 512-514 (2002).
7. M. Mueller, J. Squier, and G.J. Brakenhoff, "Measurement if femtosecond pulses in the focal point of a high-numerical-aperature lens by two-photon absorption," Opt. Lett. **20**, 1038-1040 (1995).
8. Franco Quercioli, Bruno Tiribilli, Massimo Vassalli, and Francesca Sbrana, "Autocorrelator designs for nonlinear optical microscopy," Opt. Eng. **45**, (2006).
9. Vadim V. Lozovoy, Igor Pastirk, and Marcos Dantus, "Multiphoton intrepulse interference. IV. Ultrashort pulse spectral phase characterization and compensation," Opt. Lett. **29**, 775-777 (2004).
10. David N. Fittinghoff, Jeff A. Squier, C. P. J. Barty, John N. Sweetser, Rick Trebino, and Michiel Mueller, "Collinear type II second-harmonic-generation frequency-resolved optical gating for use with high-numerical-aperture objectives," Opt. Lett. **23**, 1046-1048 (1998).
11. Rebecca Chadwick, Erik Spahr, Jeff A. Squier, and Charles G. Durfee, "Fringe-free, background-free, collinear third-harmonic generation frequency-resolved optical gating measurements for multiphoton microscopy," Opt. Lett. **31**, 3366-3368 (2006).
12. R. Trebino, *Frequency-Resolved Optical Gating: The Measurement of Ultrashort Laser Pulses* (Kluwer Academic Publishers, Boston, 2002).
13. David N. Fittinghoff, Andrew C. Millard, Jeffery A. Squier, and Michiel Mueller, "Frequency-Resolved Optical Gating Measurement of Ultrashort Pulses Passing Through a High Numerical Aperture Objective," IEEE J. Quantum Electron. **35**, (1999).
14. W. Amir, T. A. Planchon, C. G. Durfee, J. A. Squier, P. Gabolde, R. Trebino, and M. Mueller, "Simultaneous visualizations of spatial and chromatic abberations by two-dimensional Fourier transform spectral interferometry," Opt. Lett. **31**, 2927-2929 (2006).
15. Zs. Bor, Z. Gogolak, and G. Szabo, "Femtosecond-resolution pulse-front distortion measurement by time-of-flight interferometry," Opt. Lett. **14**, 862-864 (1989).

#84121 - $15.00 USD Received 14 Jun 2007; revised 19 Jul 2007; accepted 21 Jul 2007; published 27 Jul 2007

16. J. Jasapara, and W. Rudolph, "Characterization of sub-10-fs pulse focusing with high-numerical-aperture microscope objectives," Opt. Lett. **24**, 777-779 (1999).
17. Pamela Bowlan, Pable Gabolde, Aparna Schreenath, Kristen McGresham, and Rick Trebino, "Crossed-beam spectral interferometry: a simple, high-spectral-resolution method for completely characterizing complex ultrashort pulses in real time," Opt. Express **14**, 11892-11900 (2006).
18. Cl. Froehly, A. Lacourt, and J. Ch. Vienot, "Time Impulse Responce and time Frequency Responce of Optical Pupils," Nouvelle Revue D'Optique **4**, 183-196 (1973).
19. A.C Kovaecs, K. Osvay, Bor, Zs, "Group-delay measurement on laser mirrors by spectrally resolved white-light interferometry," Opt. Lett. **20**, 788-791 (1995).
20. A.P. Kovaecs, K. Osvay, G. Kurdi, M. Gorbe, J. Klenbniczki, and Z. Bor, "Dispersion Control of a pulse stretcher-compressor system with two-dimensional spectral interferometry," Appl. Phys. B **80**, 165-170 (2005).
21. J.P. Geindre, P. Audebert, S. Rebibo, and J.C. Gauthier, "Single-shot spectral interferometry with chirped pulses," Opt. Lett. **26**, 1612-1614 (2001).
22. D. Meshulach, D. Yelin, and Y. Silbergerg, "Real-Time Spatial-Spectral Interference Measurements of Ultrashort Optical Pulses," J. Opt. Soc. Am. B **14**, 2095-2098 (1997).
23. Kazuhiko Misawa, and Takayoshi Kobayashi, "Femtosecond Sangac interferometer for phase spectroscopy," Opt. Lett. **20**, (1995).
24. M.L.M Balistreri, H. Gersen, J.P. Korterik, L. Kuipers, and N.F. van Hulst, "Tracking Femtosecond Laser Pulses in Space and Time," Science **294**, (2001).
25. M.L.M Balistreri, J.P. Korterik, L. Kuipers, and N.F. van Hulst, "Phase Mapping of Optical Fields in Integrated Optical Waveguide Structures," J. Lightwave Technol. **19**, 1169 (2001).
26. H. Gersen, J.P. Korterik, N.F. van Hulst, and L. Kuipers, "Tracking ultrashort pulses through dispersive media: Experiement and theory," Phys. Rev. E **68**, 026604 (2003).
27. H. Gersen, E.M.H.P. van Dijk, J.P. Korterik, N.F. van Hulst, and L. Kuipers, "Phase mapping of ultrashort pulses in bimodal photonic structures: A window on local group velocity dispersion," Phys. Rev. E **70**, 066609 (2004).
28. M. Kempe, U. Stamm, B. Wilhelmi, and W. Rudolph, "Spatial and temporal transformation of femtosecond laser pulses by lenses and lens systems," J. Opt. Soc. Am. B **9**, 1158-1165 (1992).
29. Max Born, and Emil Wolf, *Principles of Optics* (Cambridge University Press, New York, 1999).
30. "OSLO Optical Design Program," (Lambda Research Corporation, 2004).
31. John A. Buck, *Fundamentals of Optical Fibers* (John Wiley & Sons, Inc., New Jersey, 2004).

1. Introduction

Almost all applications of ultrashort pulses require focusing them. Generally, the highest possible intensity is desired, and this is achieved when the pulse is undistorted in both space and time, so that it has a transform limited time duration and a diffraction limited focused spot size. Unfortunately, lenses and lens systems suffer from a wide variety of aberrations, and theoretical studies have shown that very complex spatio-temporal distortions can occur at a focus due, due to, for example, spherical and chromatic aberrations [1-4]. When aberrations are present, even with perfect material-dispersion compensation, the pulse can be distorted and far from transform and diffraction limited at the focus.

Thus a simple temporal measurement of the focused pulse is far from sufficient. For the same reason, a simple spatial measurement is also far from sufficient. The measurement must be *spatio-temporal*; that is, it must measure the spatio-temporal electric field, $E(x,y,z,t)$.

To further complicate the problem, in addition to focusing, pulse shaping is often used in applications such as nonlinear microscopy and coherent control and these pulses have complex shapes in intensity and phase vs. frequency. In this case, the pulse at the focus could also be very complicated in both space *and* frequency [5, 6]. Therefore, a technique that can measure the spatio-temporal electric field with high spatial and spectral resolution is needed.

Although techniques are available for measuring focused pulses in space or time separately, none of these can measure the spatio-temporal electric field. Autocorrelators are available for determining the rough pulse duration at the focus [7, 8] with no phase or spatial information. With some nonlinear-optical pulse measurement techniques, the lens in question can be used as the focusing lens in the pulse-measurement device, so that the temporal electric field after the lens is measured [9-13]. Unfortunately, all such measurements average

#84121 - $15.00 USD Received 14 Jun 2007; revised 19 Jul 2007; accepted 21 Jul 2007; published 27 Jul 2007

over all spatial dimensions at the focus, so that no spatial information is obtained (there is one exception in which minimal, qualitative spatial information was obtained [13]). Linear interferometric techniques for measuring spatial and temporal information have been introduced, but these only measure collimated pulses [14-16]. Therefore, if a focused pulse is to be characterized using these techniques, it must first be recollimated and this is usually done with the same lens that was used to focus it. In this case, the electric field of the focused pulse can only be inferred indirectly from the measurement of the recollimated beam by assuming that the phase of the lens is half of the phase obtained by double-passing the lens (which is only true if the alignment is perfect).

In this paper, we introduce a simple technique for directly measuring the complete spatio-temporal electric field at and near the focus of an ultrashort pulse. To our knowledge this is the first technique in which the spatio-temporal field, $E(x,y,z,t)$, is directly measured for a focusing pulse. From a typical measurement using our device, a movie can be made of the pulse focusing, showing its intensity and color vs. space and time.

To make these measurements we use a slightly modified version of a device that we recently introduced, called SEA TADPOLE, or Spatial Encoded Arrangement for Temporal Analysis by Dispersing a Pair of Light E-fields [17]. SEA TADPOLE is an experimentally simple and high-spectral-resolution implementation of spectral interferometry (SI) [18]. A SEA TADPOLE measurement is made by crossing and spectrally resolving two pulses in which one is a previously characterized reference pulse (which we measure using FROG or GRENOUILLE [12]) and the other is the (unknown) pulse that we wish to characterize [19-23]. We Fourier filter the interferogram to reconstruct $E(\omega)$ of the unknown pulse. Unlike standard SI, however, the Fourier filtering is done along the spatial axis of the camera (x_c), so that no spectral resolution is lost in the reconstruction and the unknown pulse can be reconstructed with the full resolution of the spectrometer. Indeed, we often even obtain *better* spectral resolution than that of the spectrometer [17]. To make SEA TADPOLE experimentally easy to use, the reference and unknown pulses each enter the device through single-mode optical fibers.

Because the entrance to SEA TADPOLE is an optical fiber, it naturally measures pulses with high spatial resolution, and, in particular, it can measure them at a focus, although collimated pulses can be measured as well. If the entrance fiber for the unknown pulse has a mode size smaller than the smallest spatial structure of the focused spot size of the unknown pulse, then $E(\omega)$ can be measured at one position (x, y, z) and then the fiber can be scanned in x, y, and z until $E(\omega)$ has been measured at all spatial points at and near the focus, resulting in $E(x,y,z,\omega)$. Inverse-Fourier-transforming to the time domain yields $E(x,y,z,t)$. Doing this, it is possible to watch the pulse focusing. We refer to this technique as scanning SEA TADPOLE.

While scanning SEA TADPOLE bears some resemblance to the method of interferometric photon tunneling scanning microscopy (PTSM) there are some key differences between the two methods [24-27]. Both methods involve sampling or spatially resolving the unknown field with an optical fiber (or an NSOM probe in the case of PTSM) and then interferometrically recombining it with a reference pulse for each position of the sampling fiber. While interferometric PSTM operates in the space and time domains scanning SEA TADPOLE operates in the space and frequency domains. Interferometric PSTM has primarily been used to measure propagating pulses in photonic structures while scanning SEA TADPOLE is intended for measuring focusing pulses.

2. Details of the method

To use SEA TADPOLE to measure $E(\omega)$ at one point in space, we temporally overlap and couple the reference and signal pulses separately into short single-mode fibers, as shown in

#84121 - $15.00 USD Received 14 Jun 2007; revised 19 Jul 2007; accepted 21 Jul 2007; published 27 Jul 2007

Fig. 1. One focal length after the fibers, we place a spherical lens (of focal length f) to collimate the light diverging from the fibers. Because each of the fibers is slightly displaced from the optic axis (each by a distance $\pm d$), the collimated beams cross, yielding horizontal interference fringes that are recorded with a digital camera. The beams also pass through a diffraction grating and a lens, so that wavelength is mapped to the horizontal position of the camera to yield the 2D SEA TADPOLE trace $S(\omega,x_c)$.

To reconstruct $E_{unk}(\omega)$ from this trace, we Fourier filter the interferogram along the x_c axis and then divide out the reference field yielding the unknown pulse field $E_{unk}(\omega)$. Because the Fourier filtering is done with respect to x_c and k_c, rather than ω and its conjugate pseudo-time variable, no spectral resolution is lost in this reconstruction. On the other hand, even though the SEA TADPOLE trace is two-dimensional, all of the unknown beam's spatial information is lost in the fiber, so that only $E_{unk}(\omega)$ (of the sampled spatial region of the beam) is constructed from a single SEA TADPOLE trace. For more details about the SEA TADPOLE experimental setup and retrieval, see reference [17].

To measure the unknown pulse as a function of both time and space, we simply scan the position of the unknown-pulse input fiber in x, y, and z and measure many traces, assuming that the input pulse train remains stable throughout the measurement, resulting in $E(x,y,z,\omega)$. See Fig. 1.

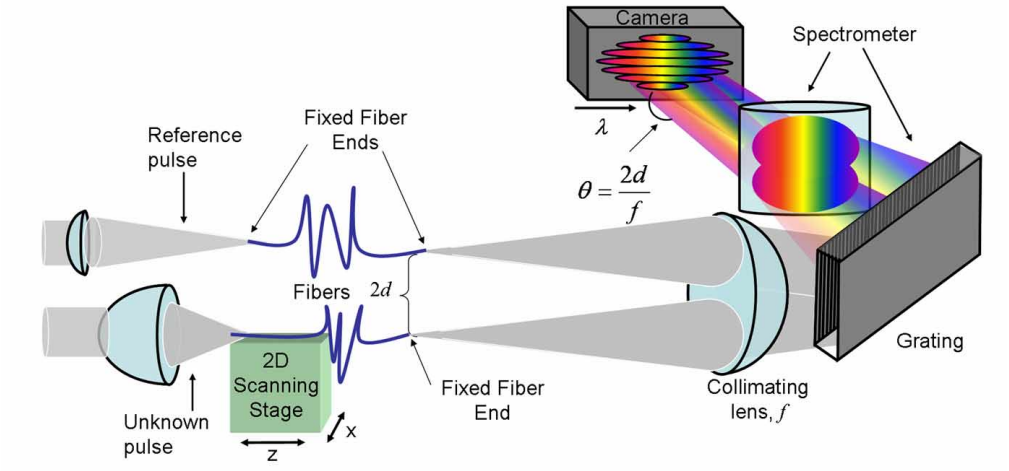

Fig. 1. Experimental setup for scanning SEA TADPOLE: The reference and unknown pulses enter the device via single-mode fibers. At the output of the fibers in the horizontal dimension, the light is collimated and then spectrally resolved at the camera using the grating and the cylindrical lens. In the vertical dimension, the light emerging from the two fibers crosses at a small angle and makes horizontal spatial fringes at the camera. With a single interferogram obtained in this way, $E(\omega)$ is measured at one position. To measure $E(x,y,z,\omega)$ of the focusing unknown pulse, the unknown pulse's entrance fiber is scanned in x, y, and z.

When the unknown fiber is moved to different longitudinal positions (z), we readjust the delay stage so that the pulses again temporally overlap (this is done by our data acquisition computer program).

As discussed previously [17, 26], the use of optical fibers in an interferometer can cause a slow drift in time in the measured absolute phase of a pulse due to small changes in the optical path lengths due to temperature fluctuations. In our measurements, the absolute spectral phase as a function of x, y, and z is the spatial phase of the pulse, so, if the absolute phase drifts faster than our scanning time, as it does here, then we are unable to measure the

#84121 - $15.00 USD Received 14 Jun 2007; revised 19 Jul 2007; accepted 21 Jul 2007; published 27 Jul 2007

spatial phase. With our current setup, however, we can measure every other aspect about a focusing pulse. In particular, we are able to measure all other phase terms, including the spectral phase and the phase terms that depend on both x or y and ω such as the radially dependent group delay and the radially dependent group-delay dispersion. Additionally we can measure the amplitude of the electric field versus x, y, z, and ω. In other interferometric techniques in which fibers are used, it has been reported that simply enclosing the interferometer in a plastic box largely eliminates the phase drift [26]. Therefore, in principle SEA TADPOLE could also easily measure the spatial phase of the pulse. In this study we are primarily interested in knowing the spatio-temporal couplings of a focusing pulse, such as the pulse fronts and the position-dependent spectrum, which can be measured by scanning SEA TADPOLE without stabilizing the interferometer, so we have not done this.

3. Experimental results

To test scanning SEA TADPOLE, we measured ultrashort pulses focused by various lenses. We measured $E_{unk}(\omega)$ for numerous values of x and z at $y = 0$ and then Fourier transformed the measured data to the time domain to obtain $E_{unk}(x,z,t)$ (with interpolation to increase the number of data points on the time axis from 10 to 90). While we could have scanned in y as well, scanning in only one transverse dimension was sufficient to measure a pulse front with spherical and chromatic aberrations for the purpose of testing our technique.

Although we know the intensity and phase of our reference pulses (we routinely monitor the output of our laser with a Swamp Optics GRENOUILLE), in these experiments the interesting quantity for scanning SEA TADPOLE was the phase introduced by the lens. So in all of our measurements we measured the phase difference in the two arms of SEA TADPOLE with the lens in the unknown arm. Therefore the following measurements show only the effects of the various lenses for a given pulse input spot size and bandwidth.

In all of our measurements, our laser source was a KM Labs mode-locked Ti:Sapphire oscillator emitting pulses with rms bandwidths of ~25 nm and centered at 800 nm. The rms spot size of the beam before each lens was 3 mm. All of the lenses studied had focal lengths of 50 mm, and we oriented the lenses so the collimated beam entered through the curved surface, which is the orientation that minimizes spherical aberration. Our optical fibers had a 5.6-μm mode field diameter. Each measurement of $E_{unk}(x,t)$ took 2-3 minutes, and the measurements at different z's were all made continuously. The remainder of the details of our set up are described in reference [17].

To confirm our measurements, we also performed simulations of pulses propagating through the various lenses used in our experiments. We performed these calculations in the manner described in references [2, 28], in which the diffraction integral in the paraxial approximation is evaluated using the appropriate lens parameters. We assumed that the input beam had no spatio-temporal distortions and that the only lens aberrations present were spherical and chromatic aberration. In these simulations, we also included the spectral phase introduced by the lens. The appropriate chromatic and spherical aberration parameters were obtained from references [1, 29] and from the ray tracing program OSLO [30]. In this way, we were able to calculate theoretical fields, $E(x,t)$, for any value of z after the lens.

The first lens that we considered was an aspheric lens made of molded PMMA, which is designed to have minimal spherical aberration, but which exhibits chromatic aberration and, group-delay dispersion (GDD). We measured and simulated $E(x,t)$ at nine different longitudinal positions, z, around the focus, where $z = 0$ corresponds to the geometric focus. See Fig. 2.

#84121 - $15.00 USD Received 14 Jun 2007; revised 19 Jul 2007; accepted 21 Jul 2007; published 27 Jul 2007

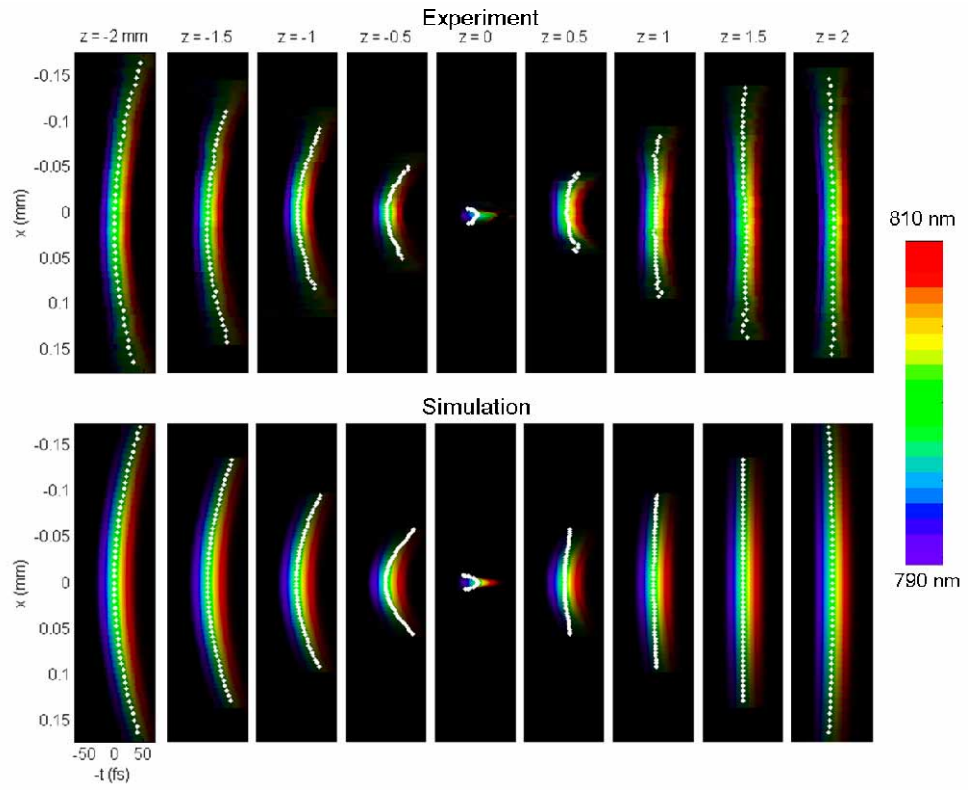

Fig. 2. $E(x,z,t)$ in the focal region of an aspheric lens. The experimental results are displayed in the top plots, and the simulations are in the bottom plots. Each box displays the amplitude of the electric field versus x and t at a distance z from the geometric focus. The color represents the instantaneous wavelength as designated by the color bar on the right. Each set of plots displays the amplitude of the electric field versus $-t$ (so that the leading edge of the pulse appears on the right) and x at a particular longitudinal distance away from the focus. The white dots display the pulse front (defined as the maximum temporal intensity at each x). The same conventions are used for the next several plots as well. In this case, as expected, chromatic aberration causes a flat pulse front to occur after the focus, at about $z = 1.5$ mm.

In the absence of dispersion and aberrations, the instantaneous wavelength would be the same everywhere in space and time so that the above plots would be uniformly green (and black where the pulse intensity is low). GDD and aberrations, on the other hand, cause color variations. For the aspheric lens, we expect color variations due to both GDD and chromatic aberration, but, for this particular lens, the effects of chromatic aberration are small compared to those due to GDD, so in all of the plots in Fig. 2, the redder colors precede the bluer colors, as expected when material dispersion is present.

While chromatic aberration plays only a small role in the pulse temporal phase, it does become evident, however, in the pulse's temporal intensity and its distortions. For a lens free of aberrations, the pulse fronts are curved and perfectly symmetrical about the focus, and flat at the focus. Chromatic aberration shifts the position of the flat pulse front to a value of z after the focus, resulting in pulse fronts that are not symmetric about the focus [3]. In Fig. 2, it is clear that the pulse fronts are, in fact, not symmetric about the focus, and the pulse front is flat at $z = 1.5$ mm in both the simulation and experimental data.

The second lens we considered was an achromatic doublet in the form of a meniscus lens consisting of a biconvex BAFN10 lens cemented to a concave-convex SF10 lens. This lens

#84121 - $15.00 USD Received 14 Jun 2007; revised 19 Jul 2007; accepted 21 Jul 2007; published 27 Jul 2007

was designed to be free of chromatic aberrations for visible light. The measurements and simulations of the focusing pulses are shown in Fig. 3.

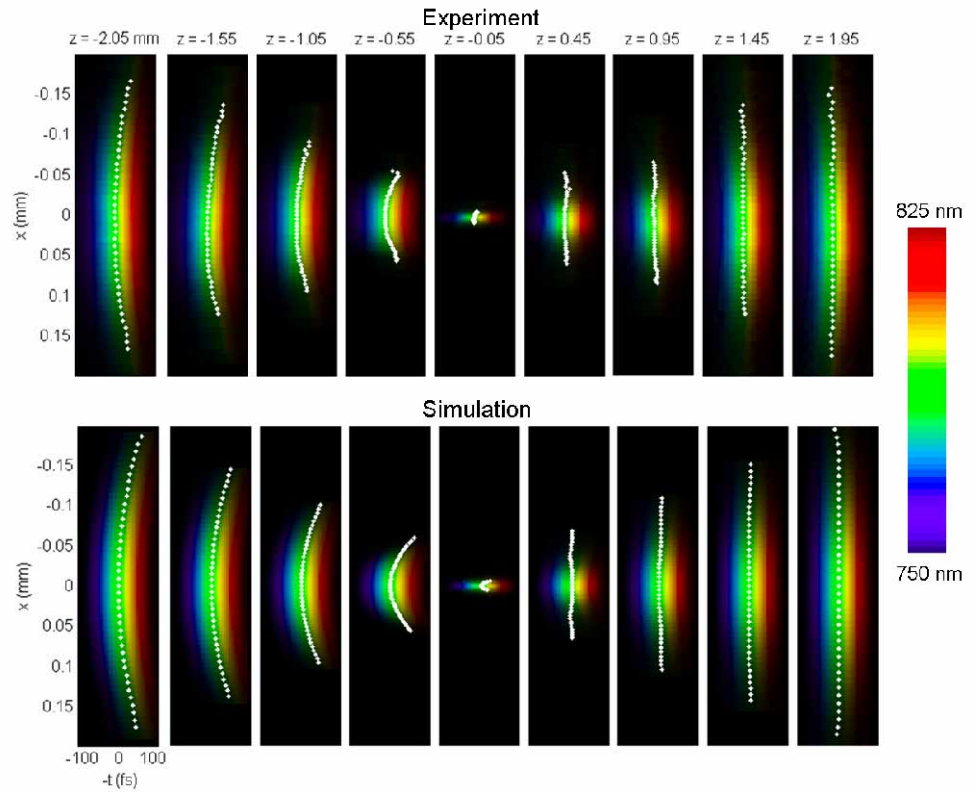

Fig. 3. $E(x,z,t)$ in the focal region of an achromatic doublet designed for visible light. Significant GDD is apparent due to the thickness of the lens. Because this lens was designed for the visible, and not 800 nm, the pulse fronts are not symmetric about the focus, revealing that some chromatic aberration is also present.

In Fig. 3, most of the color variation is again due to the GDD of the lens. Because the doublet is very thick (9.8 mm) and, made of very dispersive glass, it introduces significant GDD, and this lengthens the pulse by about three times more than the aspheric lens does (using rms temporal width of the pulse averaged over x). Also, the pulse fronts are not symmetric about the focus, revealing the presence of chromatic aberration.

We included both spherical and chromatic aberrations in the simulations of this lens. While the two lenses in the doublet do not manage to cancel out the chromatic aberration, they also greatly reduce the spherical aberration, and no noticeable effects of it can be seen in data shown in Fig. 3.

In the next set of measurements, we measured the focus using a BK7 plano-convex lens. The results for this lens are shown in Fig. 4.

#84121 - $15.00 USD Received 14 Jun 2007; revised 19 Jul 2007; accepted 21 Jul 2007; published 27 Jul 2007

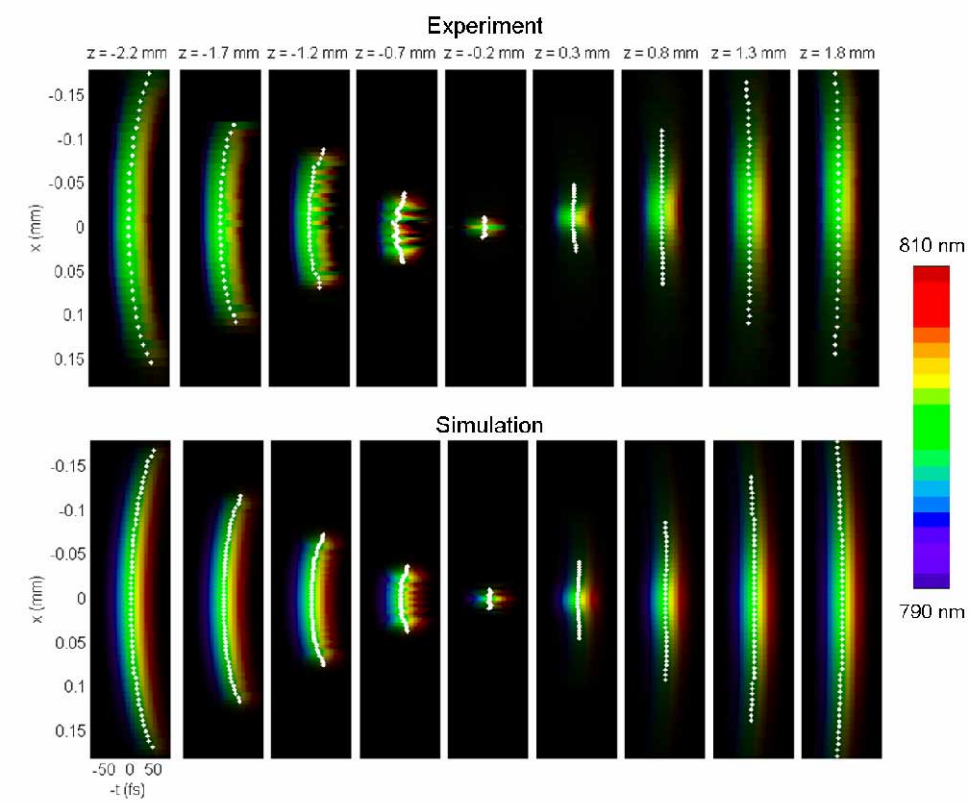

Fig. 4. $E(x,z,t)$ in the focal region of a plano-convex lens. The spherical aberrations introduced by this lens result in ripples in the spatial profile that are particularly visible at z = -0.7mm.

This lens contains noticeable amounts of both chromatic and spherical aberration. The most striking feature is the ripples in the spatial profile before the focus mainly at z = -0.7 mm. According to our simulations, the spherical aberration introduced by this lens increases the focused rms spot size by almost a factor of two. Just as with the two previous lenses, the asymmetrical pulse fronts with respect to the focus are a result of chromatic aberration. The pulse-front term introduced by spherical aberration has the opposite sign of that due to chromatic aberration [2]. As a result, the flat pulse front occurs closer to the focus than it does for the aspheric lens, when no spherical aberration is present. Just as with the two previous lenses, most of the color variation in this data is due to the GDD introduced by the BK7 glass.

In the case of spherical aberration, the focus is not well defined in position z. To determine the actual value of z for the focus in the measurements, we picked the value that resulted in the best match between the simulations and the experiments. Here, as in all of the measurements, z = 0 refers to the location of the geometric focus.

There is a small discrepancy between the simulations and experimental data, in the color, or chirp. In our simulations, we used the center thickness of the lens in the spectral phase. It is possible that we made the measurement slightly off axis (so y was not exactly equal to 0), so that the part of the beam that we were measuring did not pass through quite as much glass. Other than this minor discrepancy, the measurements are in good agreement with the simulations

In our final experiment, we measured the focal region of a plano-convex ZnSe lens. In this measurement, we felt that it would be helpful if we cancelled out most of the material

#84121 - $15.00 USD Received 14 Jun 2007; revised 19 Jul 2007; accepted 21 Jul 2007; published 27 Jul 2007

dispersion so that the effects of the lens aberrations would appear more clearly. Because SEA TADPOLE measures only the spectral phase *difference* between its two arms, we were able to cancel out the dispersion of the lens by placing a ZnSe plate whose thickness was equal to the center thickness of the lens into the reference arm. Because the radius of curvature of this lens is so large (71.46 mm), this flat plate accurately cancelled out the lens material dispersion. As a result, this set of measurements shows what distortions would remain at the focus after perfect material dispersion compensation using, for example, an ideal pulse compressor or a 1D pulse shaper before the lens.

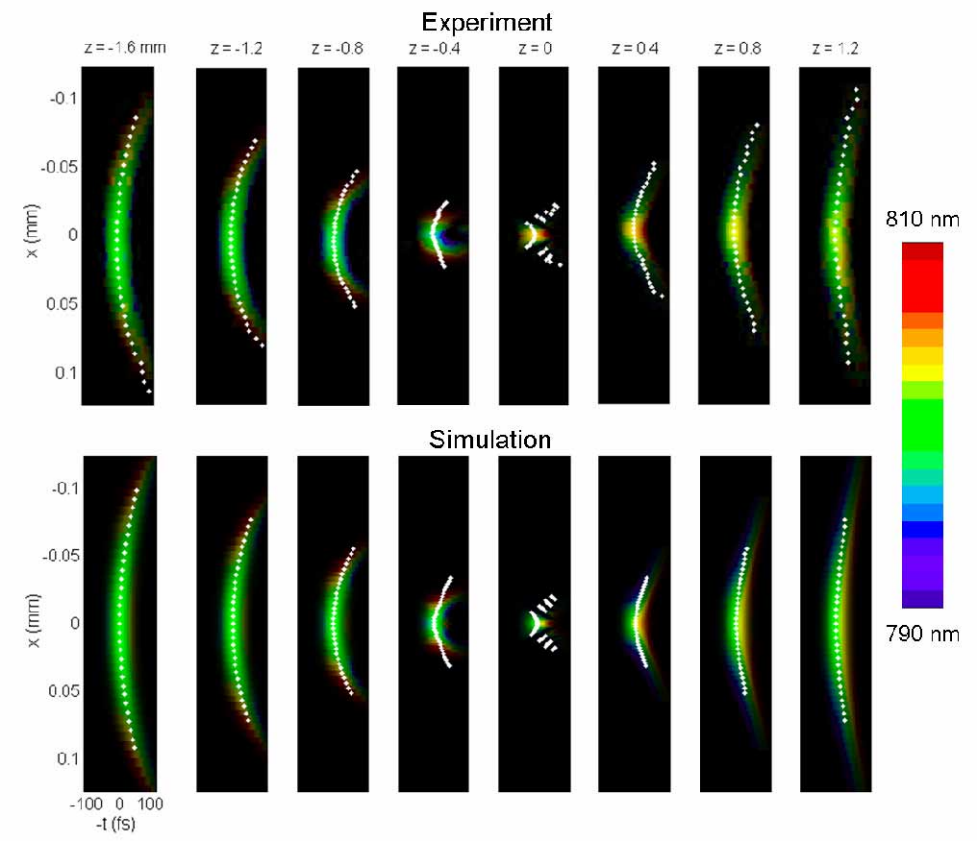

Fig. 5. $E(x,z.t)$ in the focal region of a ZnSe lens with chirp compensation. In these plots, all of the color variation is due to chromatic aberration.

The results are shown in Fig. 5. While the ZnSe lens has much more chromatic aberration than the other lenses (~ 5 times that for PMMA and BK7 using the chromatic aberration coefficient as derived in reference [3]), it actually has less spherical aberration than the BK7 lens (by a factor of about 2.5 using the spherical aberration coefficient from reference [1]). Therefore, essentially all of the distortions and color variations seen in the data are due to chromatic aberration. For this lens, even if the spectral phase of the pulse at the focus is constant, the pulse duration is still 29% longer at the focus (with a bandwidth of 25 nm) than the transform-limited pulse duration—due to the chromatic aberration.

As with the previous lenses, the pulse fronts are asymmetric about the focus due to the chromatic aberration. For this lens, the flat pulse front occurs 6.5 mm after the focus, which is out of the range of our data. At the focus, the chromatic aberration results in some ripples,

#84121 - $15.00 USD Received 14 Jun 2007; revised 19 Jul 2007; accepted 21 Jul 2007; published 27 Jul 2007

which are marked with the white dots. Note that, before the focus, the redder colors have a larger spot size, and they are ahead in time. Similarly, the pulse is bluer closer to $x = 0$. Both of these effects occur because chromatic aberration causes the bluer colors to focus before the redder colors.

To better show the distortions present in this pulse, we have produced a movie of it. See Fig. 6.

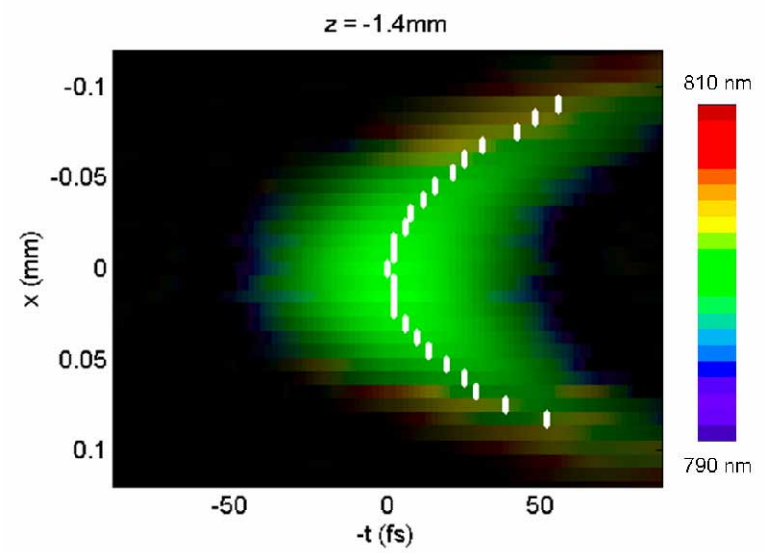

Fig. 6. (1.22 MB) Movie of the focusing pulse from a ZnSe lens with dispersion compensation: In this movie each frame shows $E(x,t)$ at a different z starting a z = -1.4 mm and stopping at z = 1.6 mm. As in the earlier plots, the white dots display the pulse front, and the color indicates the instantaneous frequency as shown by the color bar. Note that near the geometric focus (z = 0), the instantaneous wavelength changes from blue to red as a function of z, which is expected for chromatic aberration.

The movie consists of 16 measurements $E(x,t)$ at different values of z, which we interpolated along the z axis to yield 114 frames. These images range from z = -1.4 mm to z = +1.6 mm. Observe the color of the pulse close to z =0 (where the spot size is minimal), and note that it changes from blue, to green, to yellow, and finally to red, which is due to chromatic aberration.

The input beam that we used was the pulse directly out of our oscillator without spatial filtering in order to avoid seeing any aberrations from the lenses in the spatial filter in our measurements. We assumed that the input beam was relatively free of aberrations, and, because the agreement between our simulations and experiments is generally good, it is evident that this assumption is largely correct. For example, if the input beam had had chromatic aberrations that were comparable in size to those introduced by the lenses, then the flat pulse front in Fig. 3 would not have occurred close to the z = 1.5 mm plane. It is also obvious that very little spherical aberration is present in the input beam because signs of spherical aberrations (ripples in the intensity versus x) are not present in all of our data. By the same logic it is clear that the lens was well aligned, meaning that the beam passed through the center of the lens and that the lens was not tilted with respect to the beam's path. If this had not been the case, then aberrations such as coma and astigmatism would be present in the measurements, and the measured data would not have agreed with the simulations (in which

#84121 - $15.00 USD Received 14 Jun 2007; revised 19 Jul 2007; accepted 21 Jul 2007; published 27 Jul 2007

we only included chromatic and spherical aberrations). It is possible that the small discrepancies between our measurements and simulations can be attributed to the input beam or the alignment of the lens.

4. Other issues and comments

The spatial resolution of scanning SEA TADPOLE is determined by the mode size of the unknown pulse's entrance fiber, so the mode size of the fiber must be smaller than the focused spot size of the beam that is being measured (or, more precisely, smaller than the smallest spatial structure in the beam). Also, the acceptance angle of the fiber (or the fiber's NA) must be greater than the NA of the incoming focusing pulse and as long as this is the case, all k-vectors from the part of the focusing beam that overlaps with the core will be coupled into the fiber. When single-mode fibers and Gaussian beams are used, these requirements are essentially identical. For an input Gaussian beam to be effectively coupled into a single mode fiber, the NA of the Gaussian beam must be less than the NA of the fiber. The NA for a single mode step index fiber (which is what we use) with a cutoff wavelength around 700nm is approximately equal to that of a Gaussian, which is $2\lambda/\pi d$ where d is the mode field diameter of the fiber [31]. Therefore, requiring that the NA of the fiber be greater than the NA of the focused beam is equivalent to requiring that the core size of the fiber be smaller than the spot size of the focused beam. In our present setup, we use fused silica fibers with a NA = 0.12, which sets the limit for the tightest foci that we can measure. In all of our measurements, the lens NA = 0.03. In the future, using fibers with a smaller mode size, we will be able to measure tighter foci.

As described above, as long as we use a fiber whose NA is greater than that of the focus, our fiber will accurately sample the beam. There is an additional experimental test we can do to ensure that the fiber is sampling the beam. In all of our experiments, because there is no interference occurring in the time domain, $S(x,\omega)$ summed over x's (or the total spectrum) should be the same at every z. This is equivalent to saying that the total energy of the pulse should be present at every longitudinal plane. Indeed, the rms bandwidth of the total spectra at every value of z in our experiments was the same within ±1.5 nm, and this bandwidth is the same as that of the input and reference pulse.

To align the lenses in the experiments, we first simply looked at the beam's path to make sure that it propagated in a straight line through the center of the lens. Because our technique measures all aberrations in the beam, including those due to a misaligned lens, we could then measure $E(x,\omega)$ at any plane to check the alignment more precisely. The information in this measurement could then be used to better align the lens. For example, if coma or astigmatism had been present, $S(x,\omega)$ would not have been symmetric about x. Because spherical and chromatic aberrations are functions of x^2, they cause distortions that are symmetric about x so that they are easily distinguishable from those introduced by misalignment.

Because we do not scan the reference beam's input fiber, we collect no spatial information about it, and therefore the spatial quality of the reference beam has no effect on the measurement. Also note that any aberrations introduced by the optics in SEA TADPOLE would only cause small errors in $E(\omega)$ that would be the same for every measurement of $E(\omega)$ (regardless of the of the unknown pulse's fiber location), therefore these aberrations cannot be confused with those of the lens being characterized.

5. Conclusions

We have demonstrated a technique for directly measuring the spatio-temporal electric field of a focusing pulse. To do this, we simply scan in space the entrance optical fiber of a device that we call SEA TADPOLE. To illustrate our technique, we measured $E(x,z,t)$ for an aspheric lens, an achromatic doublet, and a plano-convex lens, all having an NA = 0.03. We

#84121 - $15.00 USD Received 14 Jun 2007; revised 19 Jul 2007; accepted 21 Jul 2007; published 27 Jul 2007

also measured the focus of a ZnSe lens with chirp compensation and made a movie of the pulse focusing. To confirm our measurements, we performed simulations by numerically propagating Gaussian pulses through the lenses used in the experiments. The agreement between the simulations and experiments is good.

Acknowledgements

The authors would like to thank Ulrike Fuchs for very helpful email discussions. This work was supported by an endowment provided by the Georgia Research Alliance and NSF SBIR grant #053-9595.

#84121 - $15.00 USD Received 14 Jun 2007; revised 19 Jul 2007; accepted 21 Jul 2007; published 27 Jul 2007